9th ECCOMAS Thematic Conference on the Mechanical Response of Composites
COMPOSITES 2023
G. Catalanotti, H. Petterman and G. Pittaresi (Eds)

FREE VIBRATION ANALYSIS OF THERMALLY PRESTRESSED CONSTANT AND VARIABLE STIFFNESS LAMINATED BEAMS USING STRONG UNIFIED FORMULATION

Saheed O. Ojo[1*], Giovanni Zucco[1], Paul M. Weaver[1]

[1] Bernal Institute, University of Limerick, V94 T9PX, Castletroy, Ireland
* Corresponding Author. Saheed.Ojo@ul.ie

Keywords: Free vibration analysis, Strong Unified Formulation, prestressed variable stiffness composites

Summary: *Free vibration analysis is an essential requirement to capture the behaviour of composite structures subject to dynamic loading environment. To enhance the vibratory behaviour of composite structures, variable stiffness (VS) concept offers increased design flexibilities to tailor the structural response to meet a wide range of applications. Mechanically, the increased design space created by VS techniques leads to complexities of non-classical stiffness couplings which necessitate robust computational frameworks with enriched kinematics to predict the dynamic response accurately and efficiently. In this regard, this study proposes an enhanced differential quadrature based Strong Unified Formulation (SUF) to investigate the free vibration behaviour of thermally prestressed constant and variable stiffness composite beams. The proposed SUF model exploits the flexible kinematical description of the Theory of Unified Formulation to combine a hierarchical serendipity Lagrange-based 2D finite element (FE) with 1D differential quadrature method beam element for efficient free vibration characterisation of composite beams induced with prestress at different temperatures. The proposed SUF free vibration solutions of constant stiffness and VS beams demonstrate satisfactory accuracy and achieved improved efficiency with up to 99.9% computational savings when benchmarked against ABAQUS 3D FE solutions. Finally, a numerical study reveals that the effects of thermal prestress significantly contribute to the free vibration response of constant stiffness and VS laminated beams underscoring the importance of the study.*

1 INTRODUCTION

Application of carbon fibre reinforced plastic (CFRP) composites has received wide attention in the area of high-performance mechanical structures, e.g., aerospace, automotive, offshore etc, thanks to their high strength-to-weight and stiffness-to-weight ratios in addition to their increased design space that makes it feasible to achieve tailoring of composite materials to meet specific requirements [1, 2]. The creation of variable angle tow (VAT) technology through fibre placement technologies such as Automated Fibre Placement (AFP) [3], Tailored Fibre Placement (TFP) [4] and Continuous Tow Shearing (CTS) [5] has further expanded the design space to achieve improved response of composite structures, for example, regarding enhanced buckling response of stiffened blade panels [6] and improved aeroelastic response of composite wings [7].

In the context of application of VAT designs or laminated composites in general,

prestressing is an effective procedure to introduce internal stresses into the structure with the goal of counteracting stresses resulting from applied loads [8]. According to nonlinear finite element analysis of VAT structures [9], the inclusion of thermal curing (residual) stresses may have a beneficial effect on the buckling response of composite structures and the prestress state of VAT structures should be taken into account for accurate prediction of the buckling behaviour. This observation was further emphasised in [10] where residual stresses introduced during curing are found to be responsible for the discrepancies between experimental and theoretical predictions of the buckling load of VAT structures. On this basis, Ojo et al [11] recently investigated the effect of thermal prestress on the postbuckling behaviour of composite beams and concluded that thermal prestressing significantly affects the response of the beam subject to moderate loading, but the effect of thermal prestress becomes neutralised as the beam experiences large rotations and axial deformation caused by high loading.

Accurate determination of the vibration behaviour of composite structures is of fundamental importance in structural dynamics analysis to avoid resonances. In this regard, some of the early works centred on theoretical analysis of the vibration of composite beams with solid cross-sections were pioneered by Teoh and Huang [12,13]. In their study, Timoshenko beam kinematics was adopted to demonstrate that the wavelength of the vibration mode is significantly influenced by shear deformation and bending-torsion coupling of orthotropic beams. Later, Jensen, Crawley, and Dugundji [14] employed a Rayleigh-Ritz procedure to determine the sensitivity of the accuracy of predicted lowest three natural frequencies of an unbalanced cantilevered laminated plates to the choice of assumed mode shapes. The authors showed (with experimental validation) that the inclusion of chordwise bending is vital to successfully predict the torsional frequencies for plates with high bending-torsion stiffness coupling. Summarising these findings, Dewey et al [15] concluded that the (geometrical and material) assumptions used in theoretically characterising the cross-section generally influence the free vibration response of composite beams. This conclusion presupposes that modelling the free vibration behaviour of 3D composite beams requires high-fidelity theories that encapsulates the complex (extension-bending-shear or bending-torsion) coupling effects dictating the modal response of the laminate. Consistent with this reality, and further considering the complex anisotropy induced by variable stiffness effects (in the form of variable bending-extension, bend-twist, and shear-extensional stiffness couplings), the necessity for high-fidelity theory to examine free vibration behaviour of composite laminates becomes even more crucial with implications on the accuracy, convergence, numerical stability, and efficiency of the computational process. It is therefore imperative to seek an efficient computational tool which can accurately predict the free vibration behaviour of 3D laminated constant stiffness (SC) and VAT beam structures.

The theory of Unified Formulation (UF) [16] is a reliable tool to investigate the response of a wide range of complex structures due to the generic qualities of the kinematics adopted which allow for arbitrary expansion of displacement variables to achieve high-fidelity characterisation. In the context of beam structures, UF is characterised by three-dimensional displacement fields comprising a predetermined cross-sectional deformation often defined by hierarchical expansion functions over the cross-section, and unknown 1D global displacement fields [16]. According to many studies, UF-based models have proved effective for accurate prediction of static, buckling, dynamic and free vibration, and postbuckling responses [16-19]. As a further development to achieve spectral convergence, the theory of UF has been explored within the context of strong form systems combined with high-order numerical methods like the differential quadrature method (DQM) and radial basis function to realise efficient

predictions of linear static [20-23], dynamic [20], buckling [20] and large deflection [24-26] responses of constant stiffness and variable stiffness composite structures. In another development, UF-based strong form systems combined with the recently proposed inverse differential quadrature method (iDQM) [27-28] have shown promise of spectral convergence for linear static analysis of composite beams [29]. In consistence with the merits of UF together with the spectral qualities of DQM, this study proposes to investigate the free vibration behaviour of prestressed constant and variable stiffness composite beams using an enhanced DQM-based dynamic Strong Unified Formulation (SUF). The rest of the paper is described as follows:

Preliminaries of UF are treated in section 2 while the mathematical derivations for linear thermoelastic and prestressed dynamic SUFs are outlined in sections 3. Furthermore, in section 3, discretisation by DQM is provided followed by conversion of the dynamic system to a steady-state eigenvalue system. Numerical examples and discussion on free vibration analysis of prestressed CS and VAT composite beam structures are presented in section 4 before the concluding remarks in section 5.

2 UNIFIED FORMULATION PRELIMINARIES

The theory of Unified Formulation (UF) describes the displacement fields $[u_x, u_y, u_z]$ in the three dimensions, x-, y- and z-axes of a 3D beam composite structure (see figure 1) of length L in the cartesian coordinate system by the relation

$$\boldsymbol{u}(x,y,z) = F_\tau(x,z)\boldsymbol{u}_\tau(y), \tag{1}$$

where F_τ is the function that captures the cross-sectional deformation and can be expanded to any order τ for the enrichment of the beam's kinematical description. The cross-sectional function F_τ adopted in this study is the so-called Serendipity Lagrange expansion (SLE) function that describes the cross-sectional behaviour of the beam accurately and efficiently without the need for re-meshing or loss of numerical stability (for example, see [21-24]). The stresses $(\boldsymbol{\sigma} = [\sigma_{xx} \quad \sigma_{yy} \quad \sigma_{zz} \quad \tau_{yz} \quad \tau_{xz} \quad \tau_{xy}]^T)$ and strains $(\boldsymbol{\varepsilon} = [\varepsilon_{xx} \quad \varepsilon_{yy} \quad \varepsilon_{zz} \quad \gamma_{yz} \quad \gamma_{xz} \quad \gamma_{xy}]^T)$ relationship is governed by

$$\boldsymbol{\varepsilon} = \boldsymbol{B}_{l_\tau}\boldsymbol{u}_\tau(y) \tag{2a}$$

$$\boldsymbol{\sigma} = \boldsymbol{C}\boldsymbol{\varepsilon} \tag{2b}$$

where $\boldsymbol{C} \in \mathbb{R}^{6\times6}$ is a 6×6 transformed material stiffness and $\boldsymbol{B}_{l_\tau}$ is the linear strain-displacement matrix (see [30] for example).

3 LINEAR THERMOELASTIC FORMULATION

In the preliminary stage, the laminated beam is subjected to residual prestress at a predefined temperature difference θ. For simplicity, the value of θ is assumed to be constant throughout the laminate. Then, the total linear thermoelastic strain in the structure under the influence of constant temperature change θ is given as

$$\boldsymbol{\varepsilon} = \boldsymbol{\varepsilon}_m + \boldsymbol{\varepsilon}_t \tag{3}$$

where $\boldsymbol{\varepsilon}_m$ and $\boldsymbol{\varepsilon}_t$ are, respectively, the global linear mechanical and thermal strains. The thermal strains in the global cartesian coordinate are explicitly expressed in the compact form as

$$\boldsymbol{\varepsilon}_t = -\boldsymbol{\alpha}\theta, \tag{4}$$

with $\boldsymbol{\alpha} = [\alpha_x \quad \alpha_y \quad \alpha_z \quad \alpha_{yz} \quad \alpha_{xz} \quad \alpha_{yz}]^T$ being the coefficient of thermal expansion and $\boldsymbol{v} = \left[v_x, v_y, v_z\right]^T$ is the displacement of the beam in the thermoelastic stage.

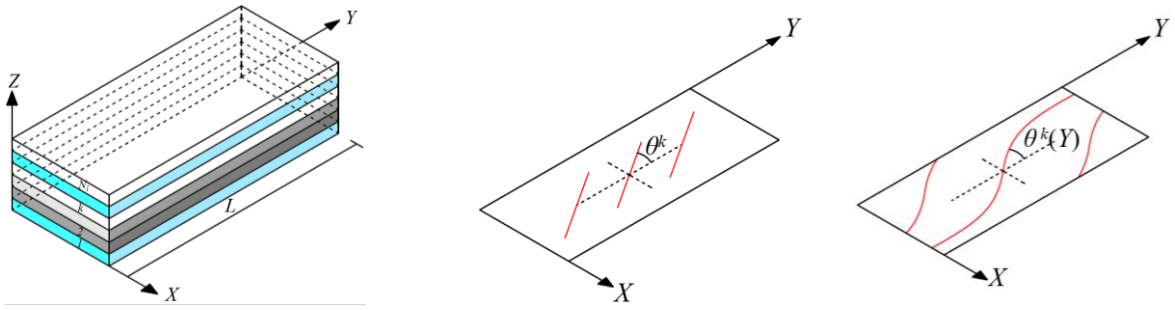

(a) (b) (c)

Figure. 1 Cartesian frame of reference for (a) laminate stack (b) constant stiffness lamina orientation, and (c) variable stiffness lamina orientation [24].

The corresponding stress $\boldsymbol{\sigma} = [\sigma_{xx} \quad \sigma_{yy} \quad \sigma_{zz} \quad \tau_{yz} \quad \tau_{xz} \quad \tau_{xy}]^T$ in the linear thermoelastic stage is expressed as

$$\boldsymbol{\sigma} = \boldsymbol{C}(\boldsymbol{\varepsilon}_m + \boldsymbol{\varepsilon}_t). \tag{5}$$

The virtual strain energy for the thermoelastic problem is obtained according to the principle of virtual work, as

$$\delta G = \int_V \delta \left(\varepsilon_{m_{xx}}\sigma_{xx} + \varepsilon_{m_{yy}}\sigma_{yy} + \varepsilon_{m_{zz}}\sigma_{zz} + \gamma_{m_{yz}}\tau_{yz} + \gamma_{m_{xz}}\tau_{xz} + \gamma_{m_{xy}}\tau_{xy}\right) \mathrm{dV} = 0, \tag{6}$$

Substituting for strains in Eq. (6) in terms of displacement $\boldsymbol{v}$ and applying partial integration-by-parts along the axial dimension y leads to (see [24-26])

$$\delta G = \int_V \delta\left(\boldsymbol{\varepsilon}^T\boldsymbol{\sigma}\right) \mathrm{dV} = \int_\Omega \delta\left(v_{x\tau}F_\tau\tau_{xy} + v_{y\tau}F_\tau\sigma_{yy} + v_{z\tau}F_\tau\tau_{yz}\right) \mathrm{d}\Omega\Big|_{y=0}^{y=L} + \int_V \delta\left(v_{x\tau}\left[F_{\tau_x}\sigma_{xx} + F_{\tau_z}\tau_{xz} - F_\tau\frac{\partial\tau_{xy}}{\partial y}\right] + v_{y\tau}\left[F_{\tau_x}\tau_{xy} - F_\tau\frac{\partial\sigma_{yy}}{\partial y} + F_{\tau_z}\tau_{yz}\right] + v_{z\tau}\left[F_{\tau_z}\sigma_{zz} - F_\tau\frac{\partial\tau_{yz}}{\partial y} + F_{\tau_x}\tau_{xz}\right]\right) \mathrm{dV} = 0 \tag{7}$$

By further substituting for stresses in terms of displacements, the thermoelastic strain energy in a compact form becomes

$$\delta G = \delta\boldsymbol{v}_\tau^T \underbrace{\int_\Omega F_\tau\bar{\boldsymbol{C}}\boldsymbol{B}_{l_s}\mathrm{d}\Omega}_{\boldsymbol{\Pi}_{l_{\tau s}}} \boldsymbol{v}_s\Big|_{y=0}^{y=L} \boldsymbol{v}_s + \int_L \delta\boldsymbol{v}_\tau^T \underbrace{\int_\Omega\left(\bar{\boldsymbol{B}}_{l_\tau}^T\boldsymbol{C}\boldsymbol{B}_{l_s} - F_\tau\boldsymbol{Q}\boldsymbol{B}_{l_s}\right)\mathrm{d}\Omega}_{\mathbf{K}_{l_{\tau s}}}\boldsymbol{v}_s\mathrm{d}y -$$

$$\delta\boldsymbol{v}_\tau^T \underbrace{\int_\Omega F_\tau\bar{\boldsymbol{C}}\boldsymbol{\alpha}\mathrm{d}\Omega}_{\boldsymbol{\Pi}_{\alpha_\tau}}\theta\Big|_{y=0}^{y=L} - \int_L \delta\boldsymbol{v}_\tau^T \underbrace{\int_\Omega\left(\bar{\boldsymbol{B}}_{l_\tau}^T\boldsymbol{C}\boldsymbol{\alpha} - F_\tau\bar{\boldsymbol{Q}}\boldsymbol{\alpha} - F_\tau\bar{\boldsymbol{C}}\boldsymbol{\beta}\right)\mathrm{d}\Omega}_{\mathbf{K}_{\alpha_\tau}}\theta\mathrm{d}y, \tag{8}$$

where

$$\boldsymbol{\beta} = \frac{\partial\boldsymbol{\alpha}}{\partial y}, \qquad \boldsymbol{Q} = \frac{\partial\boldsymbol{C}}{\partial y}, \qquad \bar{\boldsymbol{C}} = \boldsymbol{R}\boldsymbol{C}, \qquad \bar{\boldsymbol{Q}} = \boldsymbol{R}\boldsymbol{Q}, \qquad \boldsymbol{R} = \begin{bmatrix}0 & 0 & 0 & 0 & 0 & 1\\ 0 & 1 & 0 & 0 & 0 & 0\\ 0 & 0 & 0 & 1 & 0 & 0\end{bmatrix}. \tag{9}$$

The explicit expression for the terms $\overline{\boldsymbol{B}}_{l_\tau}$ is given in [11]. It should be noted that the terms containing $\boldsymbol{Q}$ and $\boldsymbol{\beta}$ are responsible for inducing variable stiffness effects in the laminated beam. As such, these terms vanish for constant stiffness laminates. The governing equations and the boundary conditions for the thermoelastic problem are consequently derived from Eq. (8) as

$$\mathbf{K}_{l_{\tau s}}\boldsymbol{v}_s - \mathbf{K}_{\alpha_\tau}\theta = 0, \tag{10a}$$

$$\boldsymbol{\Pi}_{l_{\tau s}}\boldsymbol{v}_s - \boldsymbol{\Pi}_{\alpha_\tau}\theta\big|_{y=0}^{y=L} = 0, \tag{10b}$$

Equation (10) represents one-dimensional governing system of equations and boundary conditions of the thermoelastic problem which can be expanded to any order τ, s for high-fidelity prediction of the residual prestress. In a compact form, Eq. (10) reads

$$\mathbf{K}_{\tau s}\boldsymbol{v}_s - \mathbf{f}_\tau = \mathbf{0} \tag{11}$$

Equation (11) can be expanded and assembled layer-wise to form the global system of equation for the thermoelastic problem.

3.1 Dynamic Strong Unified Formulation for thermally prestressed beam

After the initial thermal prestress $\boldsymbol{\sigma}_p \in \mathbb{R}^{6\times 1}$, the composite beam is investigated for free vibration. The total stress $\boldsymbol{S}$ in the structure while accounting for the effect of thermal prestress $\boldsymbol{\sigma}_p$ is given as

$$\boldsymbol{S} = \boldsymbol{S}_m - \boldsymbol{\sigma}_p(\boldsymbol{v}) \tag{12}$$

where $\boldsymbol{v}$ is thermoelastic-induced displacement computed from Eq. (11). The terms subscripted with m represent mechanical-load induced variables while the terms subscripted with p are prestress related. According to the principle of virtual displacement, the virtual work equilibrium relations for the modal response of the prestressed 3D laminated beam can be expressed in the form

$$\delta L_{in} + \delta L_m - \delta L_p = 0 \tag{13}$$

where δL_{in}, δL_m, and δL_p are, respectively, the virtual inertial work, virtual strain energy, and virtual work done due to prestressing which are computed through the relation

$$\delta L_{in} = \delta \boldsymbol{u}_\tau^{\mathrm{T}} \int_V F_\tau \rho_s F_s \,\mathrm{d}\Omega \ddot{\boldsymbol{u}}_s \tag{14a}$$

$$\delta L_m = \int_V \delta \boldsymbol{u}_\tau^T \left(\boldsymbol{B}_{l_\tau}^T \boldsymbol{S}_m\right) \,\mathrm{dV} \tag{14b}$$

$$\delta L_T = \int_V \delta \boldsymbol{u}_\tau^T \left(\boldsymbol{B}_{nl_\tau}^T \boldsymbol{\sigma}_p\right) \,\mathrm{dV} \tag{14c}$$

where $\boldsymbol{B}_{l_\tau}^T$ and $\boldsymbol{B}_{nl_\tau}^T$ are linear and nonlinear strain displacement matrices whose formulae can be found in [11]. After substituting Eq. (14) into Eq. (13) and applying partial integration by parts while noting Eq. (2), the displacement-based strong form of the governing equation for dynamic response of the prestressed beam is realised as

$$\delta \boldsymbol{u}_\tau^T \left(\underbrace{\int_\Omega F_\tau \overline{\boldsymbol{C}} \boldsymbol{B}_{l_s} \mathrm{d}\Omega}_{\boldsymbol{\Pi}_{l_{\tau s}}} + \underbrace{\int_\Omega \mathrm{diag}\langle \overline{\boldsymbol{B}}_{nl1_{\tau s}}^{*T} \overline{\boldsymbol{\sigma}}_p \rangle \mathrm{d}\Omega}_{\boldsymbol{\Pi}_{p_{\tau s}}} \right) \boldsymbol{u}_s \Bigg|_{y=0}^{y=L} \boldsymbol{u}_s + \int_L \delta \boldsymbol{u}_\tau^{\mathrm{T}} \underbrace{\int_\Omega F_\tau \rho_s F_s \,\mathrm{d}\Omega}_{\mathbf{M}_{\tau s}} \mathrm{d}y \, \ddot{\boldsymbol{u}}_s +$$

$$\int_L \delta \boldsymbol{u}_\tau^T \underbrace{\int_\Omega \left(\overline{\boldsymbol{B}}_{l_\tau}^T \widetilde{\boldsymbol{C}} \boldsymbol{B}_{l_s} - F_\tau \overline{\boldsymbol{Q}} \boldsymbol{B}_{l_s}\right) \mathrm{d}\Omega}_{\mathbf{K}_{l_{\tau s}}} \boldsymbol{u}_s \mathrm{d}y - \int_L \delta \boldsymbol{u}_\tau^T \underbrace{\int_\Omega \mathrm{diag}\langle \overline{\boldsymbol{B}}_{nl2_{\tau s}}^{*T} \boldsymbol{\sigma}_p \rangle \, \mathrm{d}\Omega}_{\mathbf{K}_{p_{\tau s}}} \boldsymbol{u}_s \mathrm{d}y = \mathbf{0}. \tag{15}$$

The expressions for $\overline{\boldsymbol{B}}_{nl1_{\tau s}}^{*T}$ and $\overline{\boldsymbol{B}}_{nl2_{\tau s}}^{*T}$ are given explicitly in [11]. In addition, $\overline{\boldsymbol{\sigma}}_p = \boldsymbol{R}\boldsymbol{\sigma}_p$ is the prestress value at the beam boundary whereas $\mathrm{diag}\langle \overline{\boldsymbol{B}}_{nl1_{\tau s}}^{*T} \overline{\boldsymbol{\sigma}}_p \rangle$ and $\mathrm{diag}\langle \overline{\boldsymbol{B}}_{nl2_{\tau s}}^{*T} \boldsymbol{\sigma}_p \rangle$ are 3×3 diagonal matrices, whose diagonal terms are the components of the column vectors $\overline{\boldsymbol{B}}_{nl1_{\tau s}}^{*T} \overline{\boldsymbol{\sigma}}_p$ and $\overline{\boldsymbol{B}}_{nl2_{\tau s}}^{*T} \boldsymbol{\sigma}_p$, respectively. Therefore, considering the principle of variational calculus, the fundamental nucleus of the dynamic response of the prestressed composite beam is captured in the expression

$$\mathbf{M}_{l_{\tau s}} \ddot{\boldsymbol{u}}_s + \left(\mathbf{K}_{l_{\tau s}} - \mathbf{K}_{p_{\tau s}}(\boldsymbol{v}_s)\right) \boldsymbol{u}_s(y) = 0, \tag{16a}$$

$$\left(\boldsymbol{\Pi}_{l_{\tau s}} - \boldsymbol{\Pi}_{p_{\tau s}}(\boldsymbol{v}_s)\right) \boldsymbol{u}_s \Big|_{y=0}^{y=L} = 0, \tag{16b}$$

Readers are referred to [11] for the explicit terms that make up $\mathbf{K}_{p_{\tau s}}$ and $\boldsymbol{\Pi}_{p_{\tau s}}$. The compact form of Eq. (16) reads

$$\mathbf{M}_{\tau s} \ddot{\boldsymbol{u}}_s + \mathbf{K}_{u_{\tau s}}(\boldsymbol{v}) \boldsymbol{u}_s = \mathbf{0} \tag{17}$$

3.2 Differential quadrature method discretisation

The solution of the one-dimensional systems of equations, i.e., Eq. (11) and Eq. (17), is assumed according to differential quadrature method (DQM) approximation described in [31]. For example, a dependent variable, $\boldsymbol{u}_s$ assumes the form

$$\boldsymbol{u}_s(y) = \sum_{i=1}^N L_i(y) \boldsymbol{u}_{is}, \tag{18}$$

while higher derivatives of $\boldsymbol{u}_s$ are approximated as,

$$\left.\frac{\partial \boldsymbol{u}_s(y)}{\partial y}\right|_{y_i} = \sum_{j=1}^N a_{ij}^{(1)} \boldsymbol{u}_{js}, \qquad \text{for } i,j = 1, \dots, N, \tag{19a}$$

$$\left.\frac{\partial^2 \boldsymbol{u}_s(y)}{\partial y^2}\right|_{y_i} = \sum_{j=1}^N a_{ij}^{(2)} \boldsymbol{u}_{js}, \qquad \text{for } i,j = 1, \dots, N, \tag{19b}$$

where $L_i(y)$, $a_{ij}^{(1)}$ and $a_{ij}^{(2)}$ are weighting coefficients of the control variable, $\boldsymbol{u}_s$, their first derivative and second derivatives respectively, defined by some sets of base polynomials (see [31]). Equations (11) and (17) are subsequently generalised using Eqs. (18-19) leading to

$$\mathbf{K}_{v_{ij\tau s}} \boldsymbol{v}_{is} - \mathbf{f}_{js} = 0, \tag{20}$$

$$\mathbf{M}_{ij\tau s} \ddot{\boldsymbol{u}}_{is} + \mathbf{K}_{u_{ij\tau s}} \boldsymbol{u}_{is} = 0, \tag{21}$$

Equations (20-21) constitute the fundamental nuclei of the generalised governing system of the prestressed beam which can be expanded to any arbitrary higher order of $\tau, s = 1, \dots, \mathrm{M}$ and $i,j = 1, \dots, \mathrm{N}$ to form the global system of equations

$$\mathbf{K}_v \boldsymbol{v} - \mathbf{f} = 0, \tag{22}$$

$$\mathbf{M}\ddot{\boldsymbol{u}} + \mathbf{K}_u(\boldsymbol{v}) \boldsymbol{u} = 0, \tag{23}$$

By taking $\boldsymbol{u}(y) = \boldsymbol{u}_0(y) e^{j\omega t}$, the dynamic system, i.e., Eq. (23) can be reduced to the generalised eigenvalue system

$$[\omega^2 \mathbf{M} + \mathbf{K}_u(\boldsymbol{v})] \boldsymbol{u}_0 = 0, \tag{24}$$

where ω is the natural frequency of the beam.

4 NUMERICAL EXAMPLES

Numerical examples of free vibration response of prestressed laminated beam subject to clamped-clamped and clamped-free conditions are investigated using the proposed differential quadrature based Strong Unified Formulation (UF-DQ) in section 3. To induce thermal prestress in the preliminary thermoelastic stage of the analysis, the beam is subjected to temperature change while being held clamped at both ends. Then, in the free vibration stage, clamped-clamped or clamped-free conditions are applied accordingly. For each boundary condition, two laminates constituting constant stiffness (CS) and variable angle tow (VAT) configurations are examined at 0^oC, 50^oC and -50^oC prestress levels. The properties defining the CS and VAT laminates are given in Table 1. Essentially, the first laminate consists of a two-layer non-symmetric, cross-ply constant stiffness configuration characterised by high extension-bending coupling. The second laminate represents a two-layer non-symmetric variable angle tow configuration with the first layer steered from 0^0 at the laminate edges to 90^o at the centre of the laminate while the second layer consists of 90^o fibre orientation. The VAT laminate configuration is thus characterised by high variable extension-bending, extension-shear, and bend-twist couplings.

In the first instance, ABAQUS 3D FE benchmarks are independently obtained for the non-prestressed laminate (i.e., at 0^oC prestress) to validate the accuracy of the UF-DQ estimates. However, for 50^oC and -50^oC prestress levels, ABAQUS implementation is complicated owing to the limitation of propagating thermoelastic stresses obtained from "*ABAQUS general static step*" to free vibration procedure performed in "*ABAQUS linear perturbation step*". Consequently, a UF-based finite element (UF-FE) model is further implemented to corroborate the validity of the proposed UF-DQ solution at 50^oC and -50^oC prestress levels. In general, the UF-based models are implemented with the aid of a fifth order 2D SLE element to capture the deformation of the beam cross-section. In addition, the convergence of the UF-DQ model requires 21-noded beam element (constituting 2520 DOF) for CS and 35-noded beam element (constituting 4200 DOF) for VAT laminates, respectively, while the UF-FE model convergence requires 20 4-noded beam elements (constituting 6960 DOF) and 26 4-noded beam elements (constituting 9360 DOF), respectively, for the CS and VAT laminates. On the other hand, ABAQUS 3D FE simulation is accomplished using 43200 C3D20R 3D solid elements with a total of 573675 DOF.

Table. 1: Material, geometric, and laminate properties.

E_1 (GPa)	$E_2 = E_3$ (GPa)	$G_{12} = G_{13}$ (GPa)	G_{23} (GPa)	v_{12}	v_{13}	v_{23}
136	8.76	4.54	3.32	0.25	0.43	0.32
α_1 ($10^{-6}/^oC$)		$\alpha_2 = \alpha_3$ ($10^{-6}/^oC$)				
0.11		31.94				
Geometric properties						
Length(m)		Layer Thickness(m)	Orientations			Width(m)
2		$[0.05L]_2$	$[0^o/90^o]$			0.1L
2		$[0.05L]_2$	$[<90^o\|0^o>/<90^o\|90^o>]$			0.1L

4.1 Free vibration of non-prestressed constant and variable stiffness beams

The first four frequencies of the non-prestressed beam are reported in Table 2 and excellent agreement is recorded between the UF-DQ, UF-FE, and 3D FE models for CS and VAT laminates subject to the boundary conditions examined. This outcome demonstrates the accuracy and robustness of the UF-DQ model while also exemplifying the high fidelity of UF theory in capturing the natural frequencies of 3D beams of arbitrary lamination sequence. Due to the high anisotropy induced by the variable stiffness effects, the UF-based models require finer mesh to capture the variable extension-bending, extension-shear, and bend-twist coupling responses leading to higher computational effort to attain convergence than CS configuration.

Comparing the discrepancy between the computational efforts required by the UF-DQ and UF-FE models to reach convergence, it is evident that the UF-DQ model requires 36% and 45% of the computational effort of UF-FE model for CS and VAT laminates respectively (see Table 2). Thus, the strong form UF-DQ model exhibits improved efficiency in this regard. In any case, both UF-DQ and UF-FE models show computational savings of over 99.9% over ABAQUS 3D FE model indicating the excellent computational merits of the UF-based models.

4.2 Free vibration of prestressed constant and variable stiffness beams

The benchmarking of the UF-DQ model accuracy for prestressed analysis is accomplished with comparison to UF-FE model since ABAQUS 3D FE implementation is limited in this regard. The free vibration of the prestressed beam is investigated for prestress levels of 50^{o}C and -50^{o}C which are enough to induce significant residual stresses causing the beam to experience compression, or tension, or a combination of compression and tension from its default (undeformed) state. To a large extent, according to Table 3 and Table 4, the agreement between the UF-DQ and UF-FE models is satisfactory for all the boundary conditions and laminate sequences whether for 50^{o}C or -50^{o}C prestress levels indicating the accuracy of the UF-DQ model. Remarkably, 50^{o}C prestressing causes the CS beam to experience lower natural frequency compared to the non-prestressed case owing to the net compression experienced by 0^{o} bottom layer making the beam to become stiffer or less flexible. On the other hand, -50^{o}C prestress subject the 0^{o} bottom layer to net tension while the top 90^{o} layer experiences net compression leading to increased natural frequency since the beam is now more flexible than the non-prestressed beam. Obviously, the state of the 0^{o} bottom layer after prestressing is significant to determine the modal response of the beam eventually. In the VAT laminate case, due to the variable mechanical couplings, the middle of the beam experiences net tension (due to expansion of the beam's midpoint fixed at 90^{o} fibre orientation at the top and bottom layers) while the edges are in net compression (due to dominating mechanical effect of the 0^{o} bottom layer at the beam edges) after 50^{o}C prestress resulting in a less stiff beam. Consequently, the VAT beam vibrates at lower natural frequency. Subject to -50^{o}C, the VAT beam vibrates at a higher natural frequency due to flexibility induced by the net tensile state of the beam edges. It is thus clear that the mechanics of prestressed VAT is significantly enhanced by the presence of variable mechanical couplings which tend to control the in-plane behaviour of the laminate for improved response.

Table. 2: Natural frequencies of constant and variable stiffness beams at $0°C$ prestress level.

Clamped-Clamped condition ($\Delta T = 0°C$)						
Frequency ($\times 10^3$ rad/s)	Constant stiffness laminate (CS)			Variable angle tow laminate (VAT)		
	UF-DQ (2520)	UF-FE (6960)	3D-FE (573675)	UF-DQ (4200)	UF-FE (9360)	3D-FE (573675)
ω_1	1.1208	1.1209	1.1208	0.8917	0.8917	0.8915
ω_2	1.4448	1.4448	1.4447	1.0154	1.0134	1.0110
ω_3	2.2193	2.2194	2.2192	2.0409	2.0412	2.0409
ω_4	2.6528	2.6530	2.6529	2.3363	2.3334	2.3324
Clamped-Free condition ($\Delta T = 0°C$)						
ω_1	0.2051	0.2048	0.2048	0.1383	0.1384	0.1384
ω_2	0.3077	0.3076	0.3076	0.1486	0.1487	0.1484
ω_3	1.1028	1.1027	1.1026	0.7676	0.7680	0.7679
ω_4	1.1478	1.1483	1.1483	0.8381	0.8361	0.8348

Table. 3: Natural frequencies of constant and variable stiffness beams at $50°C$ prestress level.

Clamped-Clamped condition ($\Delta T = 50°C$)				
Frequency ($\times 10^3$ rad/s)	CS		VAT	
	UF-DQ	UF-FE	UF-DQ	UF-FE
ω_1	1.1037	1.1038	0.8592	0.8592
ω_2	1.2621	1.2622	0.9626	0.9619
ω_3	1.4498	1.4498	1.3131	1.3081
ω_4	2.6294	2.6295	2.0031	2.0033
Clamped-Free condition ($\Delta T = 50°C$)				
ω_1	0.1498	0.1495	0.0958	0.0958
ω_2	0.2800	0.2800	0.1042	0.1041
ω_3	1.0986	1.0988	0.6680	0.6683
ω_4	1.4087	1.4075	0.7323	0.7297

Table. 4: Natural frequencies of constant and variable stiffness beams at $-50°C$ prestress level.

Clamped-Clamped condition ($\Delta T = -50°C$)				
Frequency ($\times 10^3$ rad/s)	CS		VAT	
	UF-DQ	UF-FE	UF-DQ	UF-FE
ω_1	1.1375	1.1376	0.9225	0.9225
ω_2	1.4560	1.4560	1.0526	1.0504
ω_3	2.6759	2.6761	2.0821	2.0823
ω_4	2.8639	2.8640	2.3816	2.3789
Clamped-Free condition ($\Delta T = -50°C$)				
ω_1	0.2448	0.2450	0.2030	0.2031
ω_2	0.3321	0.3321	0.2187	0.2188
ω_3	1.1947	1.1952	0.8600	0.8600
ω_4	1.5840	1.5842	0.9362	0.9342

From the computational perspective, the effect of prestressing is negligible on the convergence or the numerical stability of the UF-based models whether for the CS or VAT laminates. Therefore, as observed for the non-prestressed laminate, the improved computational efficiency offered by UF-DQ model over UF-FE model is preserved to a large extent. This observation emphasises the merits of the proposed model for numerical analysis of prestressed structures.

5 CONCLUSIONS

An efficient differential quadrature-based Strong Unified Formulation (UF-DQ) has been developed in this study to investigate the modal response of 3D constant stiffness (CS) and variable angle tow (VAT) laminated beams subjected to clamped-clamped and clamped-free conditions. The analysis involves a preliminary thermoelastic procedure to induce thermoelastic residual stresses in the beam in a clamped-clamped state before examining the free vibration response of the beam. By benchmarking the predictions of the UF-DQ model with finite element-based weak Unified Formulation (UF-FE) and ABAQUS 3D FE, it is revealed that the UF-DQ model furnishes accurate outcomes with up to 55% computational efficiency over UF-FE model and up to 99.9% computational savings over ABAQUS 3D FE model for non-prestressed beam. In addition, the UF-DQ model possesses the high fidelity to satisfactorily capture the free vibration behaviour of the VAT laminates typified by variable mechanical couplings. In the presence of prestress, the nonsymmetric laminated CS and VAT beams experience thermoelastic deformation in the form of combined compression and tension which makes the beam to be stiffer or more flexible than the non-prestressed beam depending on the nature of prestress. Consequently, the beam exhibits lower frequency than the non-prestressed laminate if the beam is induced with net compression or higher natural frequency than the non-prestressed laminate if the beam is induced with net tension. Interestingly, the proposed UF-DQ model accurately and efficiently predicted this behaviour, underscoring the effectiveness of the method.

ACKNOWLEDGMENTS

The Authors would like to acknowledge funding from the Science Foundation Ireland (SFI) and Temporally VARIable COMPosite (VARICOMP) Grant No. (15/RP/2773) under its Research Professor programme.

REFERENCES

[1] Khandan R, Noroozi S, Sewell P, Vinney J. The development of laminated composite plate theories: a review. *Journal of Material Science* 47 (2012), 5901–5910.

[2] Gu JW, Dong WC, Xu S, Tang YS, Ye L, Kong J. Development of wave-transparent, light-weight composites combined with superior dielectric performance and desirable thermal stabilities. *Composite Science Technology* 144 (2017), 185–192.

[3] Lopes C, Gürdal Z, Camanho P. Tailoring for strength of composite steered-fibre panels with cut outs. *Composite Part A: Applied Science and Manufacturing* 41 (2010), 1760–1767.

[4] Gliesche K, Hübner T, Orawetz H. Application of the tailored fibre placement (TFP) process for a local reinforcement on an ‘open-hole’ tension plate from carbon/ epoxy laminates. *Composite Science Technology* 63 (2003), 81–88.

[5] Kim BC, Hazra K, Weaver PM, Potter K. Limitations of fibre placement techniques for variable angle tow composites and their process-induced defects. In: *18th international*

conference on composite materials, Jeju, South Korea (2011), 1–6.
[6] Coburn BH, Wu Z, Weaver PM. Buckling analysis of stiffened variable angle tow panels. *Composite Structures* 111 (2014), 259–270.
[7] Stodieck Z, Cooper JE, Weaver PM, Kealy P. Improved aeroelastic tailoring using tow-steered composites. *Composite Structures* 106 (2013), 703–715.
[8] https://www.merriam-webster.com/dictionary/prestress
[9] Wu, C., Gurdal, Z., & Starnes, J. Structural response of compression-loaded, tow-placed, variable stiffness panels. In 43rd *AIAA/ASME/ASCE/AHS/ASC Structures, Structural Dynamics, and Materials Conference* (p. 1512), 2002.
[10] Abdalla, M. M., Gürdal, Z., & Abdelal, G. F. Thermomechanical response of variable stiffness composite panels. *Journal of Thermal Stresses*, 32(1-2), 187-208, 2008.
[11] Ojo, S. O., Zucco, G., & Weaver, P. Large deflection analysis of thermally prestressed composite beams using strong Unified Formulation. In *AIAA SCITECH 2023 Forum* (p. 1711), 2023.
[12] Teoh, L. S., & Huang, C. C. The vibration of beams of fibre reinforced material. *Journal of Sound Vibration*, 51(4), 467-473, 1977.
[13] Teh, K. K., & Huang, C. C. The effects of fibre orientation on free vibrations of composite beams. *Journal of Sound and Vibration*, 69(2), 327-337, 1980.
[14] Jensen, D. W., Crawley, E. F., & Dugundji, J. (1982). Vibration of cantilevered graphite/epoxy plates with bending-torsion coupling. *Journal of Reinforced Plastics and Composites*, 1(3), 254-269, 1982.
[15] Hodges, D. H., Atilgan, A. R., Fulton, M. V., & Rehfield, L. W. Free-Vibration analysis of composite beams. *Journal of the American Helicopter Society*, 36(3), 36-47, 1991.
[16] E. Carrera, M. Cinefra, M. Petrolo, E. Zappino. *Finite Element Analysis of Structures through Unified Formulation*. John Wiley & Sons Ltd., West Sussex, United Kingdom, 2014.
[17] Pagani, A., Carrera, E., Large-deflection and post-buckling analyses of laminated composite beams by Carrera Unified Formulation. *Composite Structures*, Vol. 170, pp. 40, 52, 2017.
[18] Yan, Y., Pagani, A., & Carrera, E. Exact solutions for free vibration analysis of laminated, box and sandwich beams by refined layer-wise theory. *Composite Structures*, 175, 28–45. doi:10.1016/j.compstruct.2017.05.003, 2017.
[19] Carrera, E., & Zappino, E. Carrera Unified Formulation for Free-Vibration Analysis of Aircraft Structures. *AIAA Journal*, 54(1), 280–292. doi:10.2514/1.j054265, 2016.
[20] Pagani, A. *Strong-form governing equations and solutions for variable kinematic beam theories with practical applications* (Doctoral dissertation, City, University of London), 2016.
[21] Ojo, S.O., Patni, M., and Weaver, P.M. Comparison of strong and weak formulations for 3D stress analysis of composite beams. *International Journal of Solids and Structures*, Vol. 178–179, pp. 145, 166, 2019.
[22] Ojo, S.O., Weaver, P.M., 3D static analysis of patched composite laminates using a multidomain differential quadrature method. *Composite Structures*, Vol. 229, 111389, 2019.
[23] Ojo, S. O., & Weaver, P. M. Efficient strong Unified Formulation for stress analysis of non-prismatic beam structures. *Composite Structures*, 114190. doi:10.1016/j.compstruct.2021.114190, 2021.
[24] Ojo, S. O., & Weaver, P. A generalized nonlinear strong Unified Formulation for large deflection analysis of composite beam structures. *AIAA Scitech 2021 Forum*.

doi:10.2514/6.2021-0698, 2021.

[25] Ojo, S. O., Zucco, G., & Weaver, P. M. Efficient three-dimensional geometrically nonlinear analysis of variable stiffness composite beams using strong Unified Formulation. *Thin-Walled Structures*, 163, 107672. doi:10.1016/j.tws.2021.107672, 2021.

[26] Ojo, S. O., & Weaver, P. M. Geometrically nonlinear analysis of non-prismatic beam structures using strong Unified Formulation. In *AIAA SCITECH 2022 Forum* (p. 2600), 2022.

[27] Ojo, S. O., Trinh, L. C., Khalid, H. M., & Weaver, P. M. Inverse differential quadrature method: mathematical formulation and error analysis. *Proceedings of the Royal Society A: Mathematical, Physical and Engineering Sciences*, 477(2248). doi:10.1098/rspa.2020.0815, 2021.

[28] Khalid, H. M., Ojo, S. O., & Weaver, P. M. Inverse differential quadrature method for structural analysis of composite plates. *Computers & Structures*, 263, 106745, 2022.

[29] Ojo, S.O., Trinh, L.C., & Weaver, P.M. Inverse Differential Quadrature Method for 3D Static Analysis of Composite Beam Structures. VIII ECCOMAS Thematic Conference on Mechanical Response of Composites. doi:10.23967/composites.2021.099, 2021.

[30] Reddy, J. N. *A simple higher-order theory for laminated composite plates*. (1984).

[31] Shu, C. (2012). Differential quadrature and its application in engineering. Springer Science & Business Media.